Scharler R., Kuerten J.G.M., Schulze K., Obernberger I., 2007: Numerical simulation of ash particle impaction in tube bundles - A case study as a basis for a CFD based ash deposit formation model in convective heat exchangers. In: Tagungsband zum 23. Deutschen Flammentag, September 2007, Berlin, Germany, VDI-Bericht Nr. 1988, ISSN 0083-5560, ISBN 978-3-18-091988-1, pp. 299-309, VDI-Verlag Düsseldorf (Hrsg.), Germany

Numerical simulation of ash particle impaction in tube bundles
A case study as a basis for a CFD based ash deposit formation model in convective heat exchangers

Dipl.-Ing. Dr. Robert Scharler[1,2,4], Dr. J.G.M. Kuerten[3], Dr.-Ing. Kai Schulze[1], Prof. Dipl.-Ing. Dr. Ingwald Obernberger[1,2,3,4]

1) Austrian Bioenergy Centre GmbH, Inffeldgasse 21b, A-8010 Graz, Austria
   Tel.: +43/316/48130033; Fax: +43/316/4813004; E-mail: robert.scharler@abc-energy.at
2) BIOS BIOENERGIESYSTEME GmbH, Inffeldgasse 21b, A-8010 Graz, Austria
3) Department of Mechanical Engineering, Technische Universiteit Eindhoven, The Netherlands
4) Institute for Resource Efficient and Sustainable Systems, Graz University of Technology, Austria

Abstract

A CFD model considering the relevant processes during ash deposition in biomass combustion plants is being developed as efficient engineering tool. Additionally, a finite volume based CFD heat exchanger model has been developed, since it is not possible to resolve all the length and time scales of turbulent flow in the heat exchanger tube bundles of the convective boiler sections. A numerical case study based on unsteady RANS with a Reynolds-stress turbulence model and Lagrangian tracking of particles was performed in order to investigate the influence of the most relevant design and operation parameters on the deposition of coarse fly ash particles in heat exchanger tube bundles of water tube boilers and to link the deposit formation model with the heat exchanger model. Typical values for in-line tube bundle geometries of evaporators and superheaters (pitch and diameter), flue gas velocities and corresponding Reynolds numbers, Stokes numbers and corresponding particle diameters, flow angles as well as flue gas temperatures were varied. The results showed that the particle mass fraction impacted on the tubes not only depends on the Stokes number of the particles, but also on the Reynolds number. Moreover, the impaction rates depend on the flow angle, on the pitch as well as on the flue gas temperature. With these results, a look-up table for the impaction rates as a function of the influencing values investigated will be created for each tube row and implemented in the CFD based heat exchanger model in order to provide a link to the deposit formation model. With this comprehensive engineering tool under development, the prediction of ash deposit formation will then be possible in the whole boiler including the convective section.

1 Introduction and objectives

The reduction of ash deposit formation in biomass fired boilers is at present one of the most important issues for plant manufacturers and operators since ash deposits considerably lower plant efficiencies and availabilities. Therefore, a CFD model considering the relevant processes during ash deposition is being developed as efficient engineering tool ([1] and [3]). Furthermore, a finite volume based CFD heat exchanger model [2] considering the interaction of the most relevant boiler types with flow and heat transfer has been developed, since it is not possible to resolve all the length and time scales of turbulent flow in the heat exchanger tube bundles of the convective boiler sections.

In order to gain basic knowledge about coarse fly ash particle impaction on heat exchanger tube bundles as well as to couple the deposit formation model with the heat exchanger model, a numerical case study concerning the influence of the most relevant operating and design parameters on the motion of coarse fly ash particles in superheater and evaporator tube bundles of water tube steam boilers was performed within this work. In this case study the paths of fly ash particles of several diameters were tracked in the unsteady turbulent flow in a heat exchanger configuration, which is calculated within the framework of the Reynolds-

averaged Navier-Stokes equation. Typical values for in-line tube bundle dimensions (pitch and diameter), flue gas velocities and corresponding Reynolds numbers, Stokes numbers and corresponding particle diameters, flow angles as well as flue gas and tube bundle wall temperatures were applied for this case study.

2 Model description

In this chapter, a short overview about the CFD models applied is given. Furthermore, the heat exchanger tube bundle geometry investigated is described, followed by an explanation of the methodology of the case study.

2.1 Numerical model

For typical heat exchanger configurations encountered in water tube boilers, the carrier flue gas flow is characterised by high levels of turbulence in combination with large-scale unsteadiness caused by vortex shedding behind the tubes. This unsteady flow has a large influence on the motion of particles in the flow. Moreover, particle response to the flow is influenced by the anisotropy of the turbulence close to the tubes. It is known from literature [4] that simulations based on steady RANS cannot accurately predict this flow. Therefore, the numerical simulations of particle-laden turbulent flow have been carried out based on the unsteady Reynolds-averaged Navier-Stokes equation with a Reynolds-stress turbulence model. The low Reynolds number version of the turbulence model, in which the boundary layers are completely resolved and no wall functions are used, is applied. Especially close to the separation points on the tube walls, this leads to more accurate predictions of the fluid flow and hence of the particle motion.

Coarse fly ash particles were inserted at the inflow boundary starting at a time where the flow has reached a state of well-developed turbulence. The particle size distribution was determined according to measurements of entrained coarse fly ash particles with a peak of the distribution between 60 and 100 μm. Particles of six different Stokes numbers, ranging between 0.2 and 30 were considered. The Stokes number is defined as the ratio of the particle relaxation time

$$\tau_p = \frac{\rho_p d_p^2}{18\mu} \tag{1}$$

and the fluid time scale $\tau_f = d_{tube}/w_{gas}$. Here, ρ_p and d_p are the mass density and diameter of the particle, μ is the fluid dynamic viscosity of the gas, d_{tube} the diameter of the tube and w_{gas} is the inflow gas velocity. The velocity of the particles at the inflow boundary was taken equal to the incoming fluid velocity. The density of the coarse fly ash particles ρ_p was set to a typical value of 2,000 kg/m^3. Furthermore, d_{tube} is 38 mm according to section 2.2 and μ is 3.04E-05 kg/ms for a flue gas with a temperature and composition according to section 2.3. With the inflow gas velocities chosen for this study (see section 2.3) the Stokes numbers 0.2, 0.4, 1, 5, 10, 30 applied correspond to particle diameters of 20.4 μm, 28.8 μm, 45.6 μm, 102 μm, 144 μm, 250 μm for a gas velocity of 5 m/s and to 14.4 μm, 20.4 μm, 32.2 μm, 72.1 μm, 102 μm, 177 μm for a gas velocity of 10 m/s.

Particles are influenced by the flow through the drag force only. For the drag force the fluctuating part of the instantaneous fluid velocity at the particle position was determined by a discrete random walk model. In real biomass fired boilers the mass loading of particles is so small that the particles have negligible influence on the flow. Therefore, in the simulations the effect of the particles on the flow was not taken into account either.

If a particle impacts on one of the tubes it is reflected using specified normal and tangential reflection coefficients. In all simulations shown, both reflection coefficients are set to a constant value of 0.25, which agrees quite well with experimental results by Van Beek [5]. For simulations with non-uniform temperature a thermophoretic force on the particles

according to the Talbot model [6], which drives the particles in the direction of lower temperature, was implemented.

The time interval during which particles are introduced was so large, that the averaged impaction results do not depend on time anymore. Simulations ran until all particles have left the computational domain through the outflow boundary. Impacted mass fractions were calculated as a function of the number of the row in streamwise direction and as a function of Stokes number.

2.2 Geometry

For the case study, an in-line tube bundle geometry representative for superheaters and evaporators in biomass fired water tube boilers with typical values of tube diameter (d = 38 mm) and pitch (a = b = 100 mm) was chosen (Figure 1, left).

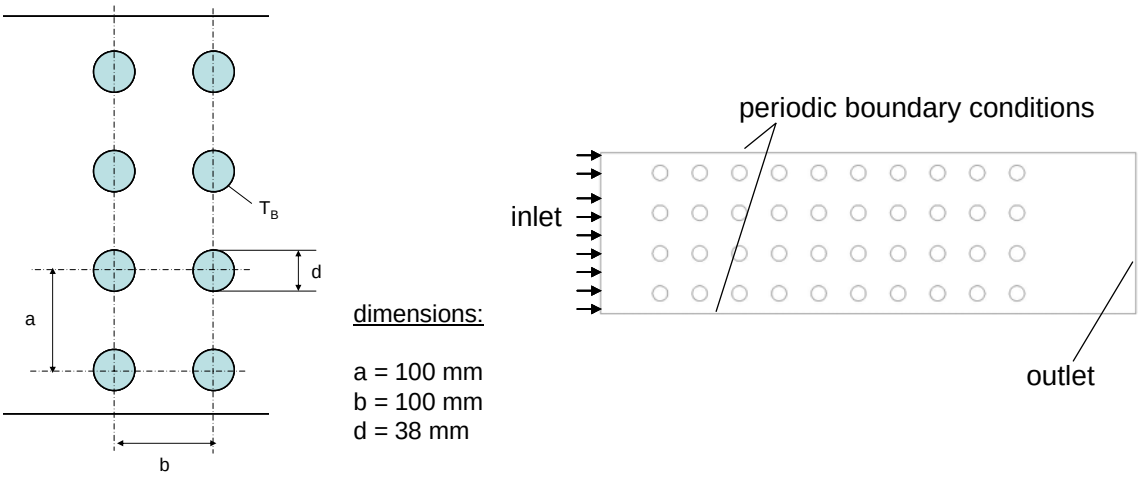

Figure 1: Geometrical setup

The width of the computational domain normal to the flow direction was set to 400 mm, whereas periodic boundary conditions were applied at the boundary (see Figure 1, right). The number of tubes in streamwise direction was taken so large that the flow between the last few tube bundles is approximately equal. It turned out that ten tubes in streamwise direction are sufficient to reach this objective. The length of the flow configurations in streamwise direction was chosen so large that the flow is developed before the first row of tubes and that no reverse flow is encountered at the outflow boundary.

For the discretisation of the geometry an unstructured grid was generated, which consists of approximately 80,000 nodes. Around each of the tubes of the bundle a structured grid was generated in order to capture the boundary layers. The first grid point in wall-normal direction was positioned at a distance of 0.1 mm from the wall, so that the value of y^+ (dimensionless wall distance) there is approximately equal to 1.

2.3 Methodology

Particle impaction rates where calculated for each of the ten tube rows in streamwise direction. For the variations within the case study, limiting values of temperatures and walls as well as velocities and inflow angels of the flue gas were chosen in order to represent a range as broad as possible of operating conditions and influencing values for superheater and evaporator tube bundles in biomass fired boilers. In all cases a constant flue gas composition typical for biomass fired boilers (ash forming vapours including SO_x and HCl as well as NO_x were neglected), consisting of oxygen, water, carbon dioxide and nitrogen was applied (Table 1).

Table 1: Chemical composition of the flue gas

species	mass fraction
O_2	0.0626
CO_2	0.1917
H_2O	0.0685
N_2	0.6772

In Table 2 an overview about the cases investigated is shown. The simulation results (impaction rates in dependence of the influencing values) will be implemented in a data base (look-up table) and interpolations will be performed to derive values for impaction rates for conditions within the range defined. However, since the number of possible variations is large due to the high number of influencing values, further simulations will be necessary in the future in order to generate more entries for the data base in order to achieve a higher interpolation accuracy and a broader validity range of the data base.

Table 3: Overview about cases investigated

case	**tube conditions**	**inlet velocity** [m/s]	**inflow angle** [°]	**Reynolds number** [-]
1	adiabatic	5	0	1975
2	non-adiabatic, 250 °C	5	0	1975
3	non-adiabatic, 250 °C	10	0	3950
4	non-adiabatic, 250 °C	5	10	1975
5	non-adiabatic, 250 °C	5	45	1975
6	non-adiabatic, 250 °C, double pitch	5	0	1975

The maximum inflow temperatures of the flue gas into the tube bundles typically occur before the first evaporator tube rows between the steam drum and the dividing wall of first and second boiler duct with a maximum value of approximately 850 °C. The corresponding evaporator tube surface temperatures in case of clean walls are about 250 °C leading to the maximum temperature difference between flue gas and walls (600 °C) and heat fluxes, respectively (non-adiabatic cases in Table 3; case 2 with an inflow velocity of 5 m/s and an inflow angle of 0° was chosen as reference case). For the purpose of interpolation, also adiabatic tube surface conditions with the same inflow temperature, inflow velocity and inflow angle as for reference case 2 where investigated (case 1), leading to 0 °C temperature difference between flue gas and tube surfaces and no heat fluxes, respectively.

The influence of inflow velocity was investigated by varying the mean velocity from 5 m/s for the reference case 2 to 10 m/s for case 3.

Since in many cases the heat exchanger tube bundles are installed after redirections of the flue gas flow, the inflow direction was investigated by varying the inflow angle from 0° for the reference case 2 to 10° for case 4 and 45° for case 5. Here it is stated, that the angle chosen for the inflow remains constant for the whole computation domain due to the periodic conditions in the flow normal direction. In reality, the flow direction aligns with the tube rows after a few tube rows, which means that the investigations for inflow angles deviating from 0° are relevant basically for the first 2 or 3 rows (or for all tube rows of staggered tube bundle configurations, which normally are not used in biomass fired boilers).

Furthermore, the influence of the pitch normal to the flow direction was investigated by halving the number of tube rows in the cross direction (case 6, same operating conditions as

for reference case 2) which is sometimes applied for fuels with high ash contents in order to prevent the tube bundles from blocking.

3 Discussion of results

Before a discussion of the particle impaction results, selected results of the fluid flow are presented. Figure 2 and Figure 3 show the mean velocity u and root mean square of the streamwise fluid velocity u' for the non-adiabatic case at an inflow velocity of 5 m/s and $\alpha = 0^{o}$. The results show that the unsteadiness of the flow results in relatively large fluctuating velocities with maximum values of more than 50% of the inflow velocity. The unsteadiness is particularly large between the tubes and in the region close to the points where the flow separates from the tubes. Moreover, it can be seen that in this non-isothermal flow the mean velocity decreases in streamwise direction due to the increased mass density.

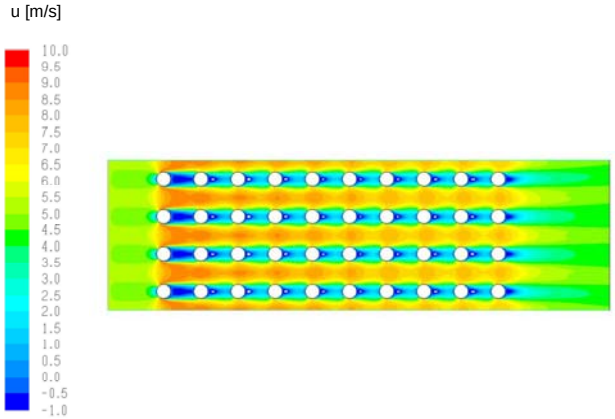

Figure 2: Mean streamwise velocity for case 2

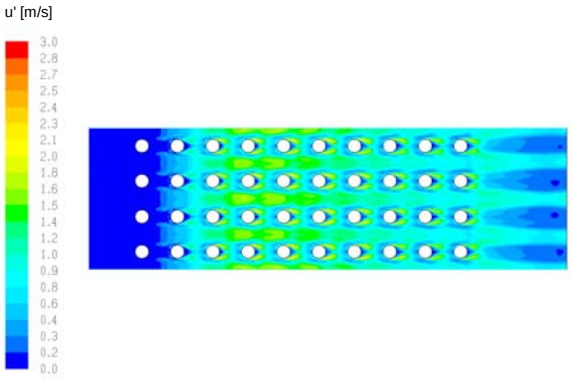

Figure 3: Root mean square of streamwise velocity for case 2

Next, significant results of particle impaction are shown. Figure 4 to Figure 9 show the ratio of particles impacted on a certain tube row and the total number of particles inserted in the flow as a function of Stokes number for the ten different tube rows, which are numbered in downstream direction. Figure 4 shows this result for the adiabatic flow and an inflow flue gas velocity of 5 m/s. The impaction rate for the first tube row corresponds well to the well known Stokes correlation for single tubes. The larger particles, with high Stokes numbers, are hardly influenced by the flow and their impaction rate is close to the ratio of the tube diameter and pitch distance of 0.38. The impaction rate of the next two rows is much smaller since these tubes are shielded by the first row. Then the impaction rates increase again (except for the very large particles) and from the fifth row onwards the results are approximately independent of the row number, especially for Stokes numbers greater than 5 to 10.

Figure 5 shows quite similar results for the non-adiabatic case. Differences to Figure 4 are small but systematic. The decreased temperature further downstream leads to somewhat higher impaction rates. Two explanations can be given for this observation. Firstly, the lower downstream temperature in the non-adiabatic case leads to a smaller dynamic viscosity and hence a larger particle relaxation time, so that particles are less able to follow the gas flow around the tubes. Secondly, the temperature gradient near the tubes leads to larger velocity fluctuations between the tubes, which can drive the particles towards the tube walls.

Furthermore, in order to investigate the effect of thermophoresis the non-adiabatic simulation of case 2 has also been performed without thermophoresis (results are not shown here). The largest differences appear at the lowest Stokes number, but for these particles the effect of thermophoresis is still very small and can be neglected compared to other effects.

Figure 6 shows the impacted mass fraction for the non-adiabatic simulation with an inflow velocity of 10 m/s. The differences between Figure 5 and Figure 6 show that particle

impaction not only depends on Stokes number, but also on Reynolds number, although this dependence is not large. With a few exceptions for the lowest Stokes number, the higher flow velocity generally results in lower impaction rates. One argument for this is related to the difference between the adiabatic and the non-adiabatic case. Since a higher flow velocity leads to a smaller mean streamwise temperature difference, the effect of the temperature difference on the particle impaction is smaller than for the smaller flow velocity. In the adiabatic case the dependence on the Reynolds number is smaller, but even then there is a very small influence of the inflow velocity of the flue gas (adiabatic results for 10 m/s are not shown here).

The impaction rates for the simulation in which the normal pitch distance is doubled are given in Figure 7. For the first tube row the impacted rates are approximately 50% smaller than for the normal pitch, which could be expected from the Stokes correlation. For the other tube rows the impaction rates follow same trends as for regular pitch but are even smaller than 50% of the impaction rates for regular pitch. Due to the larger distance between the tubes turbulence levels are much smaller there, so that the particles follow the mean fluid flow more closely.

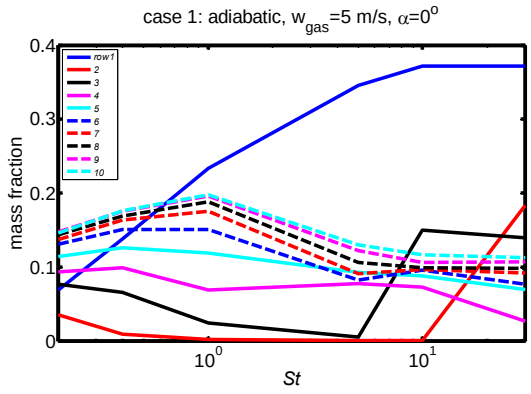

Figure 4: Impacted mass fraction for case 1

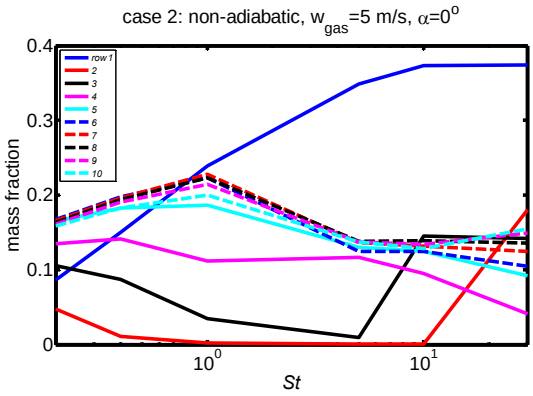

Figure 5: Impacted mass fraction for case 2

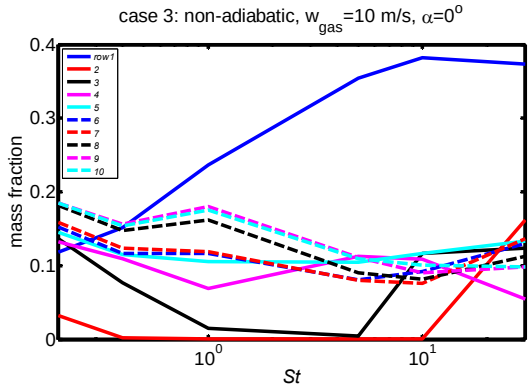

Figure 6: Impacted mass fraction for case 3

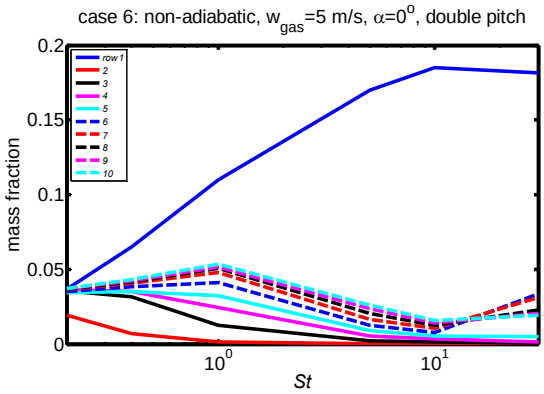

Figure 7: Impacted mass fraction for case 6

Results for $\alpha = 10^{o}$ and 45^{o} at an inflow velocity of 5 m/s (non-adiabatic) are shown in Figure 8 and Figure 9. Compared to $\alpha = 0^{o}$ the impaction rates on the first tube row increase slightly at 10^{o} and significantly at 45^{o}. This later increase can only partly be explained by the reduced apparent pitch. A second contribution comes from multiple impactions of one particle on the same tube row.

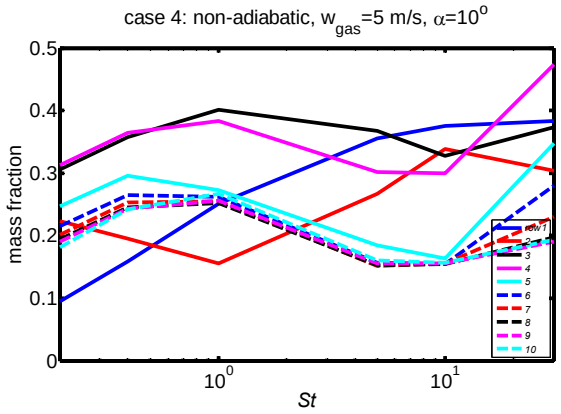

Figure 8: Impacted mass fraction for case 4

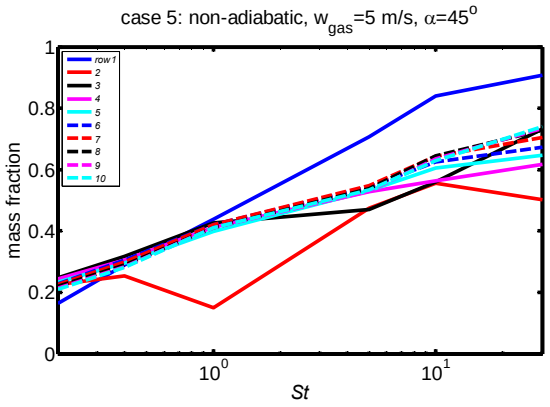

Figure 9: Impacted mass fraction for case 5

An example of this can be seen in Figure 10 where the track of a single particle with *St* = 30 which impacts twice on the first tube row is displayed. While this happens for many particles if $\alpha = 45^{o}$, it does hardly or not for $\alpha = 10^{o}$.

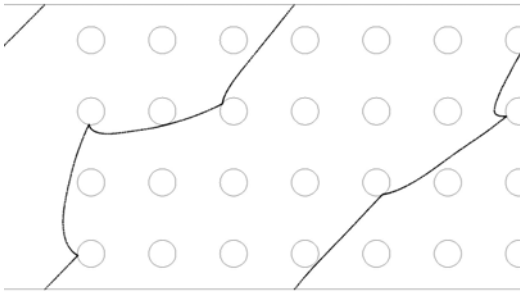

Figure 10: Track of a single particle for case 5

Another striking difference with the simulation for $\alpha = 10^{o}$ are the much higher impaction rates at the second and third tube row for $\alpha = 45^{o}$. The reason is that the shielding effect is absent at higher angles. At $\alpha = 45^{o}$ particles which pass between two tubes of the first row in contrast have a large chance to impact on the second row. For $\alpha = 10^{o}$ this explains the relatively high impaction rates at the fourth tube row. Furthermore, for $\alpha = 45^{o}$ the impaction rates hardly depend on the row number starting from the third row but a strong increase in dependence of the Stokes number can be found.

4 Summary and Conclusions

A numerical case study with a Reynolds-stress turbulence model and Lagrangian tracking of particles concerning the influence of the most relevant design and operating parameters on the impaction of coarse fly ash particles in evaporator and superheater tube bundles in biomass fired water tube boilers was performed. This work should provide a basis to gain knowledge about particle impaction on the tubes. Typical values for in-line tube bundle geometries (pitch and diameter), flue gas velocities and corresponding Reynolds numbers, Stokes numbers and corresponding particle diameters, flow angles as well as flue gas temperatures were considered within representative ranges.

Generally, for all tube bundle configurations studied an almost constant value for the impaction rates could be found after the 4th or 5th tube row. The results show that the particle mass fraction impacted on the tubes not only depends on the Stokes number of the particles, but to a lower extent also on the velocity of the flue gas. Non-adiabatic simulations with cooled tubes lead to slightly lower impaction rates for higher Stokes numbers and the second tube row onwards. Furthermore, the mean flow angle strongly influences the particle

impaction rate. While for the first tube row and 0° flow angle the impaction rates increase with the Stokes number, the impaction rates decrease first and then increase again for the 2nd and 3rd tube rows. With increasing flow angles, the particle-wall interaction is strongly augmented and the impaction rates rise with increasing Stokes numbers. If the pitch in normal direction is doubled, impaction rates are smaller by a factor of 2 for the first tube row according to the half number of tubes and even lower for the other rows due to the additionally reduced velocity fluctuations of the flow.

Next, simulations will be performed for the economiser tube bundles and a look-up table of the impaction rates as a function of the influencing variables investigated will be created for each tube row and implemented in the CFD based heat exchanger model in order to provide a link to the deposit formation model. Since the simulation results showed clear trends concerning the impaction rates, a good approximation of the impaction rates of coarse fly ash particles can be expected from this database. Concluding, by the implementation of the work performed in the heat exchanger and deposit formation models, an improved prediction of ash deposit formation will be possible in the convective boiler section.

[1] FORSTNER Martin, JOELLER Markus, DAHL Jonas, KLEDITZSCH Stefan, HOFMEISTER Georg, SCHARLER Robert, OBERNBERGER Ingwald, 2006: CFD simulation of ash deposit formation in fixed bed biomass furnaces and boilers. In: PCFD Vol. 6, Nos. 4/5 (2006), pp.248-261

[2] SCHARLER Robert, FORSTNER Martin, BRAUN Markus, BRUNNER Thomas, OBERNBERGER Ingwald, 2004: Advanced CFD analysis of large fixed bed biomass boilers with special focus on the convective section. In: Proc. of the 2nd World Conference and Exhibition on Biomass for Energy, Industry and Climate Protection, May 2004, Rome, Italy, Volume II, ISBN 88-89407-04-2, pp.1357-1360, ETA-Florence (Ed.), Italy

[3] SCHARLER Robert, JOELLER Markus, HOFMEISTER Georg, BRAUN Markus, KLEDITZSCH Stefan, OBERNBERGER Ingwald, 2005: Depositionsmodellierung in Biomasse-befeuerten Kesseln mittels CFD. In: Tagungsband zum 22. Deutschen Flammentag, Braunschweig, September 2005, VDI-Bericht Nr. 1888, ISSN 0083-5560, ISBN 3-18-091888-8, pp. 493-503, VDI-Verlag Düsseldorf (Hrsg.), Germany

[4] SIMONIN O, BARCOUDA M, 1988: Measurements and prediction of turbulent flow entering a staggered tube bundle. In: Fourth International Symposium on Applications of Laser Anemometry to Fluid Mechanics, Lisbon, Portugal

[5] TALBOT L., 1980: Thermophoresis of Particles in a Heated Boundary Layer. J. Fluid Mech., Vol. 101, No. 4 (1980), pp.737-758

[6] VAN BEEK M.C., 2001: Gas-side fouling in heat-recovery boilers. Ph.D. Thesis, Technische Universiteit Eindhoven